Nano hydroxyapatite: preparation, characterization and anti-tumor activity evaluation

H. Pan, S. Bi, Y. Yang, L. Zhang, R. Li, Y. Wu, S. He *
Department of Pharmaceutical Sciences, College of Basic Medicine and Forensic Medicine, Henan University of Science and Technology, Luoyang, 471000, China

The nano-hydroxyapatite (nHAp) displayed significant superiority in drug delivery and anti-tumor fields, which has attracted widespread attention. However, the insufficient study on the anti-tumor activity and safety restricted its application. In this study, nHAp was prepared initially by the chemical precipitation method, characterized, and the synthetic conditions were optimized. Then the anti-tumor activity were investigated against human breast cancer cells (MCF-7) via MTT test, cell colony formation test and scratch assay. What's more, in order to evaluate the safety of nHAp, MTT test was also performed on normal human liver cells (L-02). The X-ray diffractogram and Fourier transform infrared spectroscopy (FTIR) proved that nHAp was successfully prepared. And the synthesized nHAp under the optimized condition possessed uniform morphology and well dispersed particle size (212 ± 16 nm, PDI 0.178). The proliferation and migration of MCF-7 cells were inhibited in certain degree, while the proliferation of L-02 cells effected by nHAp was negligible. In conclusion, nHAp was successfully prepared and the certain degree of anti-tumor activity and safety laid the foundation for the application of nHAp as a drug carrier, especially in anti-tumor drug delivery systems.

(Received November 11, 2024; Accepted March 10, 2025)

Keywords: Nano-hydroxyapatite, Preparation, Characterization, Anti-tumor activity, Safety

1. Introduction

Nano Hydroxyapatite (nHAp) is the primary inorganic component of vertebrate bones and teeth and possess bioactivity, biocompatibility and osteoconductive properties [1]. The stock of hydroxyapatite in nature is rich and it is easily available at an affordable price [2, 3]. What's more, it is non-toxic to humans and exhibits excellent biocompatibility. All the advantages endow it extensive appliation in the medical field [4], such as bone transplant surgeries [5], implantology in dentistry [6], nano-medicine [7]. In order to achieve specific goals, especially in the field of drug delivery systems, nHAp can also be modified, such as mesoporous hydroxyapatite, PEG or iron oxide modified nHAp, etc. nHAP as a carrier can achieve the expected effects, including sustained and controlled release [8, 9], targeting [10], pH sensitivity [11], magnetic sensitivity [12], and so on.

For clinical application, outstanding carrier performance, as well as adequate biocompatibility and biosafety, are also essential [13]. What's more important, carrier free delivery systems are the most ideal state [14-16]. Based on the bioactivity and carrier application foundation of nHAp, nHAp can be considered as possessing both carrier and therapeutic functions. Hence, in order to lay the foundation for the future application of nHAp in antitumor drug delivery systems, nHAp was synthesized through a simple and feasible method, and characterized in this study. What's more, the systematic anti-tumor activity and biosafety of the synthesized nHAp were investigated.

* Corresponding author: hesuna-2008@163.com
https://doi.org/10.15251/DJNB.2025.201.265

2. Materials and methods

2.1. Materials

RPIM 1640 medium was purchased from Beijing Solarbio Science and technology Co., Ltd. And the fetal bovine serum (FBS) was obtained from Sijiqing Biologic Co. Ltd. (Hangzhou, China).

2.2. Preparation of nHAp

The nHAp was prepared according to the description in the literature with some modify [17]. Firstly, calcium nitrate ($Ca(NO_3)_2 \cdot 4H_2O$) 3.0 g and diammonium hydrogen phosphate ($(NH_4)_2HPO_4$) 1.0 g were respectively dissolved in anhydrous ethanol (A) and deionized water (B). Then the solution B was added into solution A at the specified rate of 5 ml/min, and then the formed mixture reacted for 2 h. After aging for 24 h, the supernatant was removed and the precipitate was centrifuged for 6 min at 5,000 rpm, washed three times using anhydrous ethanol and deionized water, respectively. Lastly, the precipitate was dried and ground to obtain nHAp with a well dispersed powder for further study.

2.3. Optimization of nHAp synthesis conditions

2.3.1. The effect of pH

The effect of different pH values on the synthesis of nHAp was investigated via single factor experiment. Briefly, different nHAp samples was prepared according to the description above excepting that the pH of the mixture was adjusted as 7, 8, 9, and 10 using ammonia, respectively. The nHAp synthesized under different pH conditions were analyzed via X-ray diffraction.

2.3.2. The effect of reaction temperature

The effect of different reaction temperatures on the synthesis of nHAp was also studied via single factor experiment. The reaction temperatures were set as 20, 60, and 90 °C, respectively at the optimal pH value. And the nHAp synthesized under different reaction temperatures were analyzed via X-ray diffraction.

2.4. Characterization

2.4.1. Particle size

The particle size of prepared nHAp was measured via dynamic light scattering method using the instrument (Zetasizer Nano ZSE, Malvern Instruments, UK).

2.4.2. Morphology

The morphology of the nHAp particles was scrutinized under the scanning electron microscopy (JSM 7800F, JEOL, Japan). All the samples were sprayed with gold and operated at 0.2 – 5 kV.

2.4.3. X-Ray diffraction (XRD)

The sample was scanned by X-ray diffractometer (D8 ADVANCE, Bruker Co., Germany) with Ni-filtered Cu Kα irradiation. The parameters were set as voltage: 40 kV, current: 200 mA, diffraction angle: 10 ° – 70 °, increasing step: 0.02 °. The X-ray diffractogram was recorded.

2.4.4. FTIR

The sample was tested via the FTIR spectrometer (IRTracer-100, Shimadzu Co., Japan). The samples were prepared using the potassium bromide pellets. The parameters were set as spectral range: 400 – 4000 cm^{-1}, resolution: 2 cm^{-1}. The FTIR spectrum was recorded for further analysis.

2.5. The anti-tumor activity and safety evaluation

The anti-tumor activity of nHAp were evaluated using human breast cancer cells (MCF-7) via MTT colorimetric assay, colony formation experiment and scratch assay. In order to evaluate the safety of nHAp, MTT test was also performed on normal human liver cells (L-02). MCF-7 and L-02 cells were obtained from Chinese Academy of Medical Science (Beijing, China). The two cell

lines were respectively cultured in the humidified atmosphere containing 5% CO_2 at 37 °C, and the culture medium was RPIM 1640 containing 10% FBS.

2.5.1. MTT assay

The *in vitro* cytotoxicity of nHAp was detected using the MTT colorimetric method in 96-well plates[18]. In brief, about 5000 cells suspended in 0.2 mL culture medium were seeded in one well. Until adherence, the medium was replaced with the fresh medium containing different concentrations of nHAp (100, 200, 300, 400, 500, 600, 700, 800 μg/ml). Meanwhile, a negative control group was established. MTT assay was performed following 48h incubation. The plates were examined with a plate spectrophotometer (FlexStation 3, Molecular Devices Co., USA). The wavelength was set as 570 nm. Cell inhibition was calculated as Equation 1.

$$\text{Cell Inhibition } (\%) = \frac{\text{OD}_c - \text{OD}_t}{\text{OD}_c - \text{OD}_b} \times 100\% \quad (1)$$

Here, OD_b, OD_t, OD_c were the mean absorption values of the blank wells, treated wells with serial concentrations of nHAp and the control wells, respectively. And then all the data were used to calculate the half maximal inhibitory concentrations (IC50) by SPSS 22.0.

2.5.2. Cell colony formation assay

The cell colony formation experiment was executed according to the literature [19]. Briefly, cells were seeded into 6-well plates (2×10^3 cells/well) in the form of single cell suspension solution until adherence, and then removed the medium and washed the cells for 3 times with PBS. Then cells were cultured with the fresh medium containing serial concentrations of nHAp (50, 100, 150, 200, 250 μg/ml). Meanwhile, a negative control group was established. After 2 weeks, cultivation was terminated and the cells were fixed with formaldehyde (15 min) and then stained with crystal violet (30 min). After gently rinsed with water for several minutes, the cells were taken photos.

2.5.3. Cell scratch assay

The cell scratch experiment was performed according to the literature [20]. In brief, cells were seeded in 6-well plates (2×10^5 cells/well) to culture until 90% confluence. Then a wound was created by scratching the cells using a 200-μL pipette tip. The cells were treated with different concentrations of nHAp (100, 300, 500 μg/ml) for 48 h. The cells were imaged using the inverted microscope (Olympus, Japan) at 0 and 48 h, respectively. The distance of the wound was used to analyze the scratch healing efficiency.

2.6. Statistical analysis

In the study, all the data were expressed as mean ± standard deviation (SD). and the statistical analysis was conducted via Students' *t* test (Microsoft Office 2019). $P < 0.01$ was regarded as highly significant difference and $P < 0.05$ was significant difference.

3. Results and discussion

3.1. Optimization of the synthesis conditions for nHAp

3.1.1. The effect of pH on the synthesis of nHAp

The X-ray diffraction patterns of the products synthesized at different pH values were shown in Fig. 1. It could be observed that the XRD pattern of the sample synthesized at pH 7 was inconsistent with the standard card of nHAp. However, products respectively synthesized at pH values of 8, 9, and 10 matched the standard card of nHAp. What's more, the characteristic diffraction peak for the sample synthesized at pH 10 was sharper and higher than that at pH 8 and pH 9, suggesting the higher crystallinity and purity. As the pH of the reaction system increased, dicalcium phosphate would gradually transform into octacalcium phosphate. And with the pH further raised, the transformation of octacalcium phosphate into hydroxyapatite could be occurred [21-23]. The results above showing that the pH above 8 was crucial for the synthesis of nHAp, and pH 10 was

the optimal condition for high purity and crystallinity. Thus, the pH was controlled at 10 for the synthesis of nHAp in the following study.

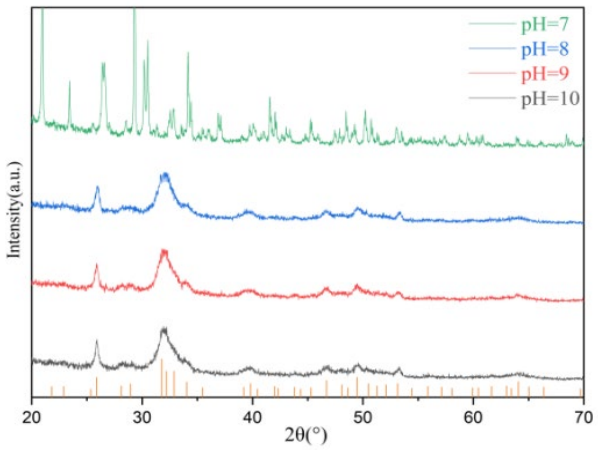

Fig. 1. The XRD patterns of the samples respectively synthesized under the condition of pH=7, 8, 9, 10 compared with the standard XRD card of nHAp (PDF#09-0432).

3.1.2. The effect of temperature on the synthesis of nHAp

The X-ray diffraction patterns of the products respectively synthesized at 20 °C, 60 °C, and 90 °C under the condition of pH 10 were shown in Fig. 2. The X-ray diffraction patterns of all the products highly matched the standard XRD card of nHAp (PDF#09-0432), meaning that nHAp could be synthesized successfully at the different temperature. However, the shape of the characteristic diffraction peaks between the samples showed clear differences. As shown in Fig. 2, when the reaction temperature increases from 20 °C to 60 °C and 90 °C, the characteristic diffraction peaks near 2θ = 30° displayed significant change. The distinct and sharp peaks emerged. Additionally, the intensity of the peaks also significantly increased. All above indicated the increased crystallinity.

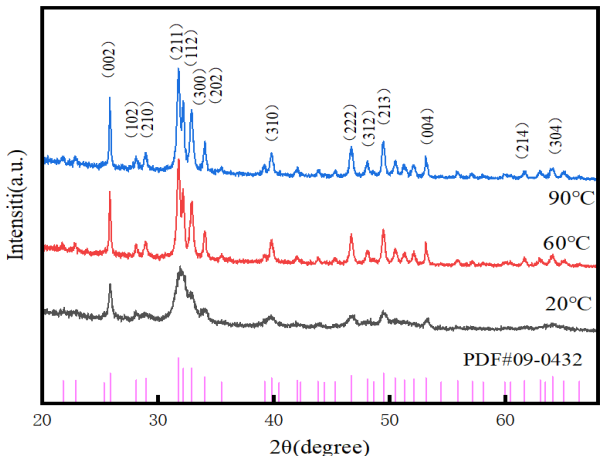

Fig. 2. The XRD patterns of the products respectively synthesized at 20 °C, 60 °C, and 90 °C compared with the standard XRD card of nHAp (PDF#09-0432).

The nucleation rate and growth rate were greatly affected by temperature and closely related to the nucleation method [24]. When the size of a nucleus reached a critical value, it would continue to grow and eventually become a stable nucleus. However, at higher temperatures, crystallization [25, 26]. Therefore, temperature not only affected the crystallinity of nHAp but also affected the particle size. Generally, increasing the temperature could promote the crystal growth of nHAp and improve its crystallinity, while the particle size of nHAp along the 002 crystal plane would increase accordingly according to Scherrer's formula [27]. In summary, the nHAp prepared at the reaction temperature of 60 °C possessed both higher crystallinity and complete crystal form.the thermal motion of molecules intensified, making it challenging to form a nucleus, or the formed nucleus became unstable. At lower temperatures, the critical nucleus size was small, leading to faster nucleation due to more

3.2. Characterization of nHAp

The nHAp was synthesized under the conditions of pH 10 and 60 °C and then characterized. As the result of DLS analysis, the average particle size of nHAp was 212 nm with a narrow distribution (PDI 0.178). And The SEM image showed that nHAp was a spindle shape (Fig. 3b). The XRD pattern of synthesized nHAp with high and sharp characteristic diffraction peaks highly matched the standard card of nHAp. As shown in Fig. 3d, the stretching vibration absorption peak of -O-H in the HAp lattice appeared at 3569 cm^{-1} [28]. The peaks at 1098 cm^{-1} was due to the asymmetric stretching vibration of PO_4^{3-} [29]. The absorption peak at 3400 cm^{-1} was due to the stretching vibration of water, indicating that the product contained a certain amount of water. The absorption peak at 1423 cm^{-1} was mainly caused by the stretching vibration of C-O, but it was very weak, indicating that there was no obvious presence of CO_3^{2-} in the product. All above results suggested that nHAp was successfully synthesized under the optimized conditions.

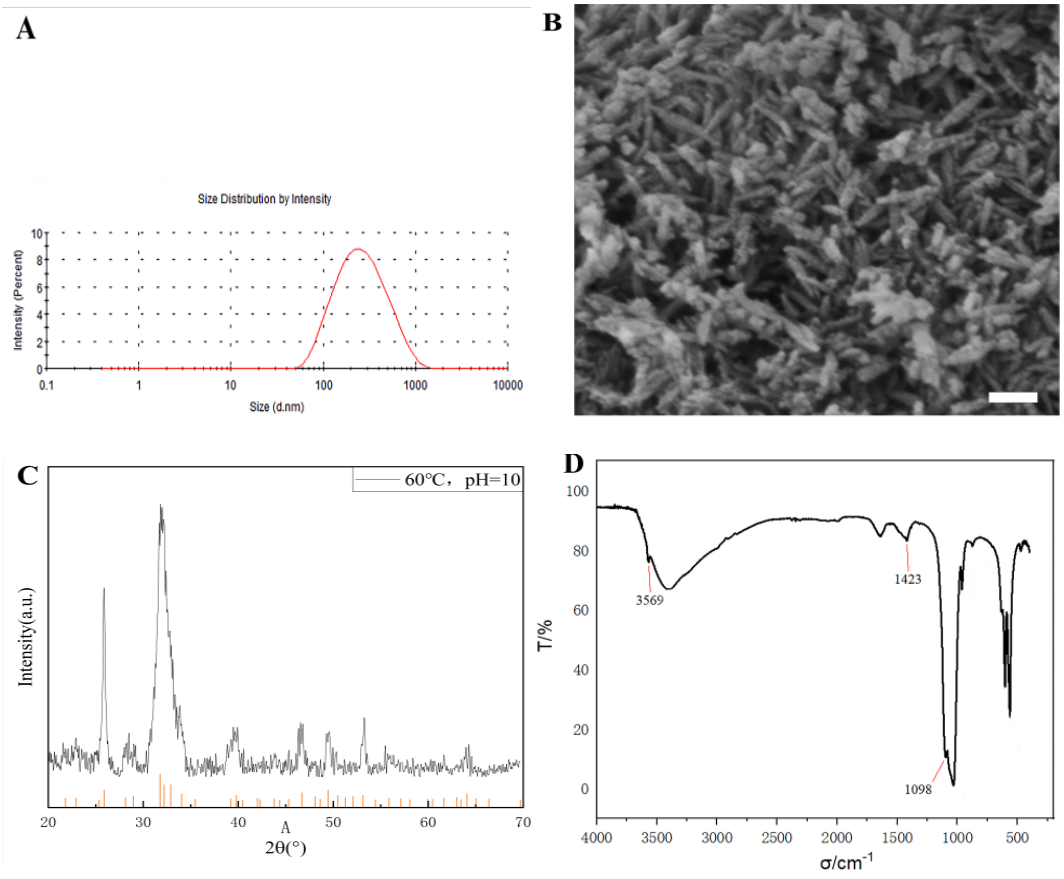

Fig. 3. Characterization of nHAp synthesized at pH=10 and 60 °C. (A: Particle size and size distribution, B: SEM image, bar: 200 nm, C: XRD pattern compared with the standard XRD card of nHAp (PDF#09-0432), D: Infrared spectroscopy).

3.3. The anti-tumor activity and safety evaluation

Generally, the MTT assay, cell clone formation experiment and cell scratch assay were commonly used to evaluate the cytotoxic effects and migration inhibition of a given substance on cells, respectively. In the study, the effects of nHAp on the proliferation of normal hepatocytes cells L-02 and breast cancer cells MCF-7 were used to evaluate the safety and anti-tumor activity of nHAp, respectively. And then the cloning and migration experiment were performed to further evaluate the anti-tumor activity of nHAp.

3.3.1. Cytotoxicity

The cytotoxicity of nHAp was evaluated via MTT method on MCF-7 and L-02 cells, respectively and the results were shown in Fig. 4. We could see that the inhibitory effect of nHAp on the proliferation of MCF-7 cells was obvious. The inhibitory rate reached 57.92% at 700 μg/mL, while the inhibitory rate of L-02 cells was only 12.75%. The results indicated that nHAp possessed marked inhibitory effect on MCF-7 cells, but it was negligible on normal liver cells L-02. These results suggested that nHAp possesses certain anti-tumor activity and good safety, which was we expect.

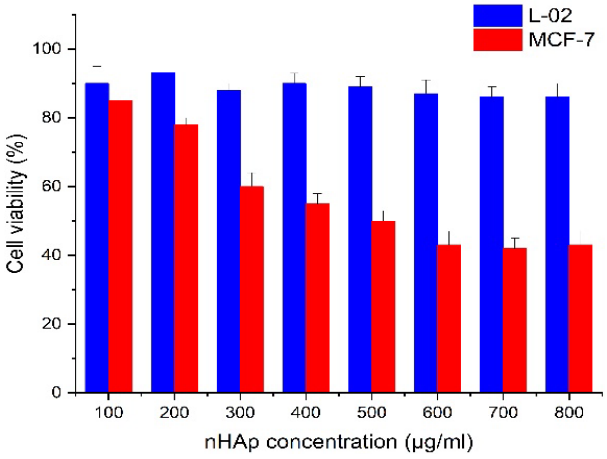

Fig. 4. The effect of nHAp on the viability of L-02 and MCF-7 cells (n=3).

Although nHAp possesses certain anti-tumor activity, the cytotoxicity was much lower than that of adriamycin, which was commonly used in clinic, and the IC50 was less than 1 μg/ml [18]. It meant that the cytotoxicity of nHAp as a single drug can't meet the clinical application, but it could play a synergistic role with drugs as a carrier.

3.3.2. Cell colony formation

Generally, the colony formation assay was used to evaluate the ability of cells to grow and form colonies, aiming to indicate the viability and proliferation. In the study, the effect of nHAp on the cloning ability of MCF-7 cells was analyzed via the plate cloning experiment. The results shown in Fig. 5 displayed that the number of cell clones decreased gradually with the increase of nHAp concentration compared with the control group. Clonal formation experiment was an effective method to determine the proliferation ability of single cell. Because it was not that every cell attached to the wall could proliferate and form a clone, and the cells that formed a clone must possesses adhesion ability and proliferation activity [30, 31]. Therefore, the clone formation rate could reflect the dependence and proliferation ability of cell population. The results above indicated that nHAp could inhibit the proliferation and cloning of MCF-7 cells, and the phenomenon was concentration dependent. The results were also confirmed by MTT results.

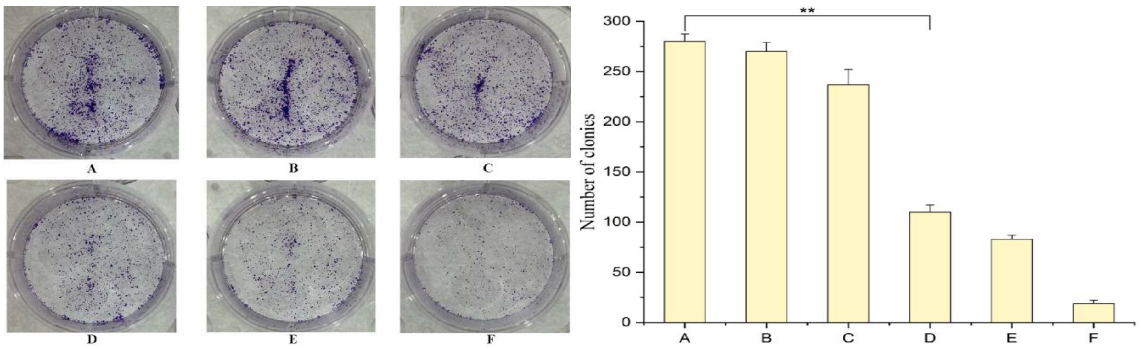

*Fig. 5. The effect of nHAp on clone formation of MCF-7 cells (A: Control; B: 50 μg/mL nHAp; C:100 μg/mL nHAp ; D: 150 μg/mL nHAp; E: 200 μg/mL nHAp ; F: 250 μg/mL nHAp, n=3, **P<0.01).*

3.3.3. Cell scratch test

The effect of nHAp on the migration of MCF-7 cells was studied by scratch experiment. The results showed that the scratch width in the control group significantly reduced after 48 h of incubation compared with all the groups treated with nHAp. And the change of scratch in different groups was dose dependent. With nHAp concentration increased, the change of scratch gradually decreased (Fig. 6). It meant that the scratch healing speed of MCF-7 cells gradually slowed down. The results displayed that nHAp could inhibit the migration of MCF-7 cells.

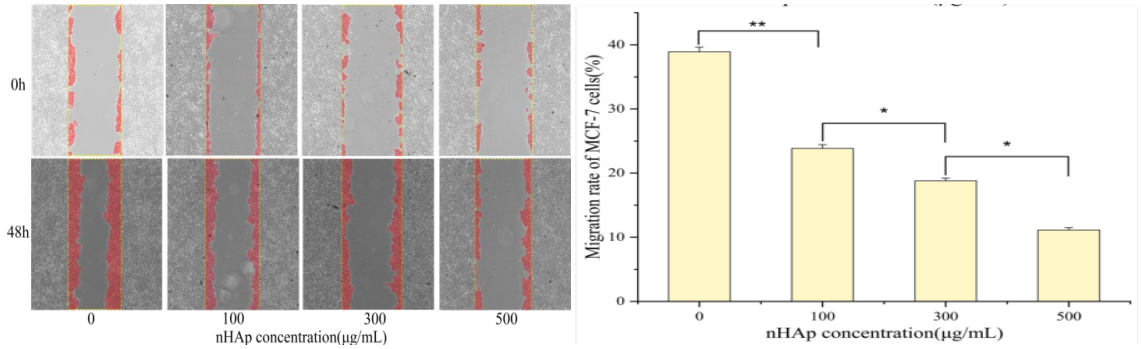

*Fig. 6. The effect of nHAp on the migration of MCF-7 cells (n=3，*P<0.05，**P<0.01).*

4. Conclusion

In the study, nHAp was successfully synthesized via a simple and feasible chemical precipitation method under the optimized conditions. The synthesized nHAp was uniformly spindle-shaped with high crystallinity, high purity and well dispersed particle size. The favourable anti-tumor activity and biosafety of nHAp were also proved by cell experiments. The study laid the foundation for the further research and application of nHAp as a drug carrier, especially in anti-tumor drug delivery systems.

Acknowledgements

This work was supported by the Training Plan for Young Backbone Teachers in Henan University of Science and Technology (No.13450005), the Innovation and Entrepreneurship Training Program for College Students of Henan University of Science and Technology (No.2024523) and the experimental technology fund of Henan University of Science and Technology (No. SY-2223231218). The authors are grateful for the financial support.

References

[1] A. Rajabiyan, L. Vaccaro and A. Ahmady, Trop. Life Sci. Res. 34(2), 243 (2023); https://doi.org/10.21315/tlsr2023.34.2.12

[2] M. S. Sri et al., Biomass Convers. Bior. 14(16), 19393 (2023); https://doi.org/10.1007/s13399-023-04008-z

[3] V. M. Rao et al., Key Eng. Mater. 962, 53 (2023); https://doi.org/10.4028/p-5m2V0j

[4] A. Abraham et al., Biomass Convers. Bior. (2023); https://doi.org/10.1007/s13399-023-04929-9

[5] M. Sayed et al., J. Non-Crystal. Solids 610, (2023); https://doi.org/10.1016/j.jnoncrysol.2023.122327

[6] K. Pajor, L. Pajchel and J. Kolmas, Materials 12(17), (2019); https://doi.org/10.3390/ma12172683

[7] S. Nouri, R. Roghanian and G. Emtizi, Iran. J. Med. Microbiol. 15(4), 369 (2021); https://doi.org/10.30699/ijmm.15.4.369

[8] S. A. Seyhan et al., J. Aust. Ceram. Soc. 58(655), 1231 (2022); https://doi.org/10.1007/s41779-022-00739-w

[9] Y. Ryabenkova et al., Langmuir 33(12), 2965 (2017); https://doi.org/10.1021/acs.langmuir.6b04510

[10] M. S. Asghar et al., Kuwait J. Sci. 50(2), 97 (2021).

[11] Y.-H. Yang et al., J. Mater. Chem. B 1(19), 2447 (2013); https://doi.org/10.1039/c3tb20365d

[12] V. Zeyni, S. Karimi and H. Namazi, Micropor. Mesopor. Mat. 354, (2023); https://doi.org/10.1016/j.micromeso.2023.112544

[13] Y. Huang et al., J. Control. Release 362, 243 (2023).

[14] J. Zhou, et al., J. Colloid Interf. Sci. 637, 453 (2023); https://doi.org/10.21203/rs.3.rs-373238/v1

[15] Y. Li et al., Mater. Chem. Front. 5(14), 5312 (2021).

[16] J. Zhou et al., J. Colloid Interf. Sci. 637, 453 (2023); https://doi.org/10.1016/j.jcis.2023.01.091

[17] S.-C. Wu et al., Molecules 28(13), 4926 (2023); https://doi.org/10.3390/molecules28134926

[18] S. He et al., Pak. J. Pharm. Sci. 36(3), 895 (2023).

[19] J. Gonçalves et al., Int. J. Mol. Sci. 25(10), 5381 (2024).

[20] Z. Hajilou et al., Hepatoma Res. 10, 1 (2024).

[21] M. Santana Vázquez et al., Crystals 10(12), 1131 (2020); https://doi.org/10.3390/cryst10121131

[22] Y. Sugiura and K. Ishikawa, Crystals 8(5), 222 (2018); https://doi.org/10.3390/cryst8050222

[23] T. Yokoi et al., B. Chem. Soc. JPN. 93(5), 701 (2020); https://doi.org/10.1246/bcsj.20200031

[24] J. Kangas and C. Hogan, Phys. Rev. E 109(1), (2024); https://doi.org/10.1103/PhysRevE.109.014617

[25] K. Onuma et al., Acta Biomater. 125, 333 (2021); https://doi.org/10.1016/j.actbio.2021.02.024

[26] Y. Wang et al., J. Phys.: Conf. Ser. 2709(1), 012004 (2024); https://doi.org/10.1088/1742-6596/2709/1/012004

[27] A. Vashchuk, and A. Ślosarczyk, Physicochem. Probl. Miner. Process. 59(4), 174338 (2023).

[28] B. Agha, N. Hamaghareeb and F. Hussain, Cell. Mol. Biol. 69(11), 149 (2023); https://doi.org/10.14715/cmb/2023.69.11.22

[29] N. Hossain et al., Nano. (2024).
[30] O. Lucas et al., Cancer Res. 84(3), 10 (2024); https://doi.org/10.1158/1538-7445.CANEVOL23-PR010
[31] D. Naor， et al., J. Autoimmun. 2 Suppl, 3 (1989); https://doi.org/10.1016/0896-8411(89)90112-1